Routson Cody Craig (Orcid ID: 0000-0001-8694-7809)
Arcusa St&#x00E9;phanie (Orcid ID: 0000-0003-0694-9623)
McKay Nicholas P. (Orcid ID: 0000-0003-3598-5113)
Overpeck Jonathan (Orcid ID: 0000-0002-3843-9313)

**A 4500-year-long record of southern Rocky Mountain dust deposition.**

Cody C. Routson[1], Stéphanie H. Arcusa[1], Nicholas P. McKay[1], Jonathan T. Overpeck [2].

1) School of Earth and Sustainability, Northern Arizona University, Flagstaff, Arizona 86011
2) School for Environment and Sustainability, University of Michigan, Ann Arbor, MI 48109

**Key Points:**

**-**A new 4500-year-long record of natural dust deposition shows a long term decreasing trend.

**-**Drought variability, as characterized by tree-rings, is not closely linked with dust mass accumulation.

**-**Human disturbance substantially increased dust deposition since 1880.

**Abstract** Dust emissions from southwestern North America (Southwest) impact human health and water resources. Whereas a growing network of regional dust reconstructions characterizes the long-term natural variability of dustiness in the Southwest, short-term fluctuations remain unexplored. We present a 4.5-millennia near-annual record of dust mass accumulation rates (DMAR) from the southern Rocky Mountains, CO. Using micro-scanning X-ray fluorescence and a geochemical end-member mixing model, the record confirms dust increased with human disturbance beginning around 1880 CE, reversing a long-term decreasing trend potentially related to changes in effective moisture, wind, and vegetation. However, increases in DMAR do not correspond to years or periods of drought, as characterized by tree-rings. This result suggests sediment supply and transport mechanisms have a strong influence on dust deposition. The record shows the Southwest is naturally prone to dustiness; however, human disturbances have a large influence on dust emissions, which can be mitigated by changing land-use.

**Plain Language Summary** We use a sediment record to characterize the long-term

naturally driven changes in dust deposition over the past 4.5 millennia. The record shows a long-term trend toward decreasing dust deposition, which was reversed with human-induced land disturbance beginning in the middle 19th century. The long-term trend may be related to effective moisture, wind, and vegetation. Nonetheless, there appears to be little relationship between known drought events and increased dust deposition, suggesting the controls on dust deposition include factors such as sediment source and transport mechanisms acting independently of drought.

## 1. Introduction

Mineral dust deposition around the world affects biogeochemical cycles and water resources and plays a role in dust-climate feedbacks (Ballantyne et al., 2011; Krinner et al., 2006; Painter et al., 2010a). In the Southwest dust reduces mountain runoff through changes in snow-albedo, snowmelt rates, and sublimation (Hall, 1981; Derbyshire, 2007; Painter et al., 2007, 2010b, 2017; Skiles et al., 2015). Dust emissions from the Colorado Plateau and surrounding deserts are mediated by soil stability, which is influenced by human disturbances, moisture, temperature, vegetation, sediment supply, and wind strength (Munson et al., 2011; Ferrenberg et al., 2015). Erosion, from fluvial processes such as arroyo cutting and migration (Lancaster, 1997a), produce the sediment (Bullard & Livingstone, 2002) that, if unprotected by vegetation (Li et al., 2007), will be entrained from Southwestern deserts and transported by dominant westerly winds (Neff et al., 2013). Soil moisture also plays a critical role in dust emissions by mediating soil cohesion (Kok et al., 2012). Thus, projections of future Southwestern drought (Cook et al., 2015) will likely have consequences for dust production.

Whether the mechanisms controlling dust emission also apply to dust deposition is unclear. Observational evidence suggests 70% of deposition is through storms and wet deposition (e.g., Lawrence et al., 2010) that may mediate the influence of drought. Limited data preceding human interference restricts our understanding of the importance of drought on dust emission and deposition. However, unlike for the erosive process of dust emission, dust deposition is preserved in natural archives such as lakes. Dust accumulates in lakes both through direct deposition and secondarily as dust deposited on snow and soil in the watershed that can subsequently be remobilized through streams and overland flow (Ballantyne et al., 2011; Neff et al., 2008b; Routson et al., 2016b). Lake catchment characteristics controls the proportion of dust versus local material and the proportion of re-worked dust from soils in the record. Once entrained in the lake, the dust is preserved within the sediment.

A sedimentary record from Fish Lake in the southern Rocky Mountains spanning the last 3000 years shows enhanced dust concentrations during intervals of persistent drought and aridity (Routson et al., 2016a). The Fish Lake record, however, is based on dust concentrations, rather than dust mass accumulation rates (DMAR). As a result, factors such as reduced local runoff (e.g.

2

during drought) can increase the sediment dust fraction without changing dust deposition rates. Here we question the importance of drought on dust deposition by testing whether deposition is higher during drier years. We compare drought, as characterized by tree rings, to a new record of near-annual DMAR spanning the last 4,500 years from Blue Lake in the southern Rocky Mountains, CO. The Blue lake DMAR record integrates the dust fraction, sedimentation rates, and sediment density, presenting an improved estimation of past dust deposition.

## 2. Methods
### 2.1 Study site

Blue Lake (37.24°N, 106.63°W) is located in a glacially carved cirque in the southern San Juan Mountains (Figure 1). The lake is 16.2 m deep with a 0.11 $km^2$ surface area. The catchment area (0.14 $km^2$ excluding the lake surface) consists of only the surrounding hillslopes, with no inflowing creaks or streams. The lake is at 3,500 m elevation and roughly 100 m below the local upper tree line. Blue Lake is located in the Oligocene south San Juan volcanic field Conejos Formation (Lipman & Hail, 1975). The bedrock consists of vent facies including lava flows, and flow breccias of andesite, rhyodacite, and quartz latite.

### 2.2 Sediment coring

Three cores were collected from Blue Lake in 2009 and 2011 using a Universal corer. The Blue Lake cores are 247 cm (core A), 151 cm (core B), and 32 cm (core C) long respectively. The upper 10.5 cm of core A was lost during coring. The interface between the sediment surface and water was undisturbed in Cores B and C. Core C was used for $^{210}$Pb dating of the upper surface sediments, and the dust analyses were primarily conducted on core A and B. Core depths were cross-correlated using distinct marker layers in the sediment as well as total organic content characterized using loss on ignition.

### 2.3 Age and sedimentation rate modeling

Radiometric dating including $^{210}$Pb and $^{14}$C was used to constrain the ages of the sediment cores. The surface of core C was sampled at 0.5 cm intervals for $^{210}$Pb and $^{226}$Ra analysis, which was conducted at the University of Florida, Land Use and Environmental Change Institute. Measurements were made using low-background gamma counting with well-type intrinsic germanium detectors (Appleby et al., 1987; Schelske et al., 1994). The constant rate of supply model was used to calculate the sediment ages (Appleby & Oldfield, 1983), and errors were propagated using first order approximations (Binford, 1990). Radiocarbon samples were analyzed at the Accelerator Mass Spectrometer facility at the University of Arizona. The Bayesian age-depth modeling R software package BACON (Blaauw & Christen, 2011) was used to calibrate the radiocarbon ages and develop the age depth model (Figure 2). Radiocarbon ages

3

were calibrated using the IntCal13.14C calibration curve (Reimer et al., 2013). Sedimentation rates were estimated by dividing depth intervals by the accumulation time as estimated by the BACON age model.

### 2.4 Sediment density

Sediment density and total organic content were characterized using loss on ignition. Two cores were sampled at 0.25 cm intervals with 0.25 cm$^3$ samples of wet sediment. Samples were weighed, dried in crucibles at 50 °C, weighed a second time, combusted at 500 °C for 12 hours to remove organic carbon, and weighed a final time. Inorganic sediment density was computed by dividing the burned sample weight minus the crucible weight by the original sample volume (0.25 cm$^3$).

### 2.5 Geochemical analysis and dust fraction

Micro-scanning X-ray florescence (µXRF) was used to characterize the fraction of dust in Blue Lake sediment, following the methods outlined in Routson et al. (2016). Sediments were subsampled into 4.5 cm intervals and imbedded in epoxy resin. The samples were split using a diamond saw and surfaced with 400 grit sandpaper. The µXRF scans were run on an EDAX Eagle III tabletop scanning µXRF at the University of Arizona. Bedrock and dust samples were pulverized in a mortar and pestle, compressed into pellets, and run on the µXRF using the same settings as the sediment.

The geochemistry of windblown dust from the Colorado Plateau is distinct from the volcanic bedrock underlying the small Blue Lake catchment. Figure 3 shows Ti/Ca ratios versus K/Ca ratios, which are lower in the catchment bedrock than windblown dust sampled from the snow surface at Molas Pass and Wolf Creek pass in the spring of 2012. The sediment, a mixture of these two endmembers is distributed between them as the proportion of local material and dust changes. To estimate the fraction of dust in the sediments we applied a simple end-member mixing model (1) using potassium calcium ratios in the sediment, dust, and bedrock following the methods applied in Routson et al. (2016).

$$fd = \frac{\frac{K}{Ca}sed - \frac{K}{Ca}rock}{\frac{K}{Ca}dust - \frac{K}{Ca}rock} \tag{1}$$

To conceptualize the mixing model in Figure 3, we applied a mean adjustment to the sediment µXRF scan counts of K, Ti, and Ca following Routson et al. (2016). Epoxy embedded sediments have lower mean µXRF counts with respect to the compact dust and bedrock pellets. The epoxy resin, organic matter, and lower sediment density influence different element counts differently. A constant value of 40 was added to the potassium and calcium and 20 to the titanium counts to

4

illustrate the mixing model in Figure 3. We used K/Ca ratios in the mixing model to estimate the fraction of dust in sediment through time, so the adjustment has no impact on the reconstruction.

The dust sampled from the snow surface under-represents the range of variability in the sediments and many lake sediment samples fall outside both the bedrock and dust end-members (Figure 3). As a result, the mixing model (1) indicates that some of the sediments exceed 100% dust, which is not possible and creates unrealistically high mass accumulation rates. To account for this, we scale the sediment fraction by the maximum estimated fraction, forcing all sediment measurements to be less than or equal to 100% dust. We recognize that this artificial scaling, and the lack of broad enough end-members, introduces substantial uncertainty to the reconstruction. Consequently, the dust fraction is best interpreted as a relative index of dust deposition. Plausible concentrations also enable the estimation of dust mass accumulation rates that facilitate interpretation of the record and comparisons with drought records.

### 2.6 Estimating dust mass accumulation rates

Dust mass accumulation rates were estimated by multiplying each dust fraction measurement with the sedimentation rate and sediment density. The age-depth model from the BACON output and the sediment densities were linearly interpolated to the resolution of the µXRF data to facilitate continuous estimates at each interval.

### 2.7 Reconstruction uncertainties

Mixing model uncertainty in the reconstruction was estimated by randomly sampling from the geochemical dust and bedrock end-members to generate a distribution of 1000 estimates of dust mass accumulation for each depth down core. Age model uncertainty from the Bayesian age depth modeling program BACON (Blaauw et al., 2010) was also propagated into the reconstruction uncertainty intervals by reproducing the reconstruction over 1000 age-model ensembles.

### 2.8 Age uncertain dust and drought analysis

We tested the likelihood of higher dust accumulation during drought years within the context of age uncertainty using a Monte Carlo approach. The record of drought was defined over the last 2000 years using the average of the Living Blended Drought Atlas grid points in the Colorado Plateau Four-Corners region (35°N - 37°N, 106°W - 112°W) (Cook et al., 2010). The Living Blended Drought Atlas is a recalibrated data series of June-July-August Palmer Modified Drought Index (PMDI). Individual drought years were defined as PMDI < -1, non-drought as PMDI >=0. Multidecadal-length drought was defined by smoothing the PMDI with a 30-year running average and using the same drought thresholds as during individual years. The long-term

5

trend was removed from the Blue Lake DMAR reconstruction by removing the slope of a linear regression for each DMAR ensemble member. For each drought and non-drought year (and similarly for the multidecadal analysis) we compiled 1000 estimates of DMAR based on individual age ensemble members. DMAR during drought and non-droughts were compared using a Wilcox test for significant difference in the mean.

## 3. Results and Discussion

The Blue Lake cores span a duration of ca. 4,500 years (Figure 2). Sediments are fine grained, discontinuously laminated, and contain no flood or debris deposits. The laminations are sub-mm-scale and composed of organic rich and minerogenic components likely reflecting seasonally deposited clastic sediments and productivity. The end-member mixing model (Figure 3) suggests Blue Lake sediment is on average 175% dust, which is physically impossible. Figure 3 illustrates how the dust end-member, as sampled from the melting snow surface at Wolf Creek Pass and Molas Pass of the southern Rocky Mountains in 2012, under-represents the range of dust geochemistry in the sediment, and the average sediment end-member falls to the right of the average dust end-member. After forcing dust concentrations below 100%, average dust concentrations are 24%. Total organic carbon ranges between 10% and 20%. Average dry inorganic sediment density is $0.2 \text{ g/cm}^3$ of wet sediment (Figure 4D).

Blue Lake had average sedimentation rates of 0.55 mm/yr over the past 4.5 millennia (Figure 2 and 4C). The number and position of radiocarbon dates impacts the sedimentation rates, and the BACON age model creates often abrupt sedimentation rate inflections near age control points (Figure 4C). Sedimentation rates were 0.56 mm/yr between 4500 BP and 2900 BP, and 0.48 mm/yr between 2900 BP and 2300 BP. The highest sedimentation rates prior to the industrial era occurred between 2280 and 1270 BP (0.65 mm/yr), and the lowest recorded sedimentation rates occurred between 1260 and 1120 BP (0.35 mm/yr). The medieval period (ca. 1200 BP to 550 BP) had an average sedimentation of 0.50 mm/yr. Sedimentation rates were 0.45 mm/yr between 440 BP to 12 BP. Between 12 BP and -59 BP (1940 CE and 2009 CE) sedimentation rates increased to 0.71 mm/yr. It is unclear to what extent the anomalously high sediment rate peak between 1,485 and 1430 BP reflects a true change in sedimentation rate or an inflection between two radiocarbon dates at this interval.

We compare dust concentrations from Blue Lake with those of Fish Lake (4 km from Blue Lake), because accurate density measurements were not taken and thus dust accumulation rates were not calculated on Fish Lake (Routson et al., 2016). Blue Lake has a smaller catchment than Fish Lake ($0.22 \text{ km}^2$ vs $0.51 \text{ km}^2$ not accounting for the area under water), reducing the potential for dust reworking from soils at Blue Lake. Blue Lake sediments are also finely laminated and not disrupted by flood deposits or turbidites (underwater landslides), unlike Fish Lake. The temporal dust concentration variations in the Blue Lake sediment cores (Figure 4B) are broadly consistent

6

with the Fish Lake dust record. Dust concentrations are not ideal for comparison between sites because sedimentation rates and sediment density influence dust mass accumulation rates. Nonetheless, both lakes show dust concentrations were high ca. 3000 BP. Dust concentrations decreased to ca. 1500 BP in Blue Lake and ca. 1300 BP in Fish Lake. Both lakes then show slight increases in dust concentration, with Blue Lake showing an earlier increase then decline than Fish Lake during this broadly defined "Medieval" interval (ca. 1200 BP to ca. 550 BP). Both lakes show dust concentration increased with human land disturbances ca. 1880 CE and that dustiness has then decrease since the 1950's CE.

Converting the Blue Lake record to dust mass accumulation rate (Figure 4A) changes this picture. There are limitations and additional uncertainties when converting to mass accumulation rates. These primarily include uncertainties in actual dust concentrations due to limitations with the mixing model, sample measurement uncertainties in computing density with loss on ignition, and age model uncertainties influencing sedimentation rates. As noted above, sedimentation rates can have inflections associated with age control points, which in turn have a large impact on the final accumulation record. In light of these uncertainties, average dust mass accumulation rates in the Blue Lake sediment cores are 29 $g/m^2/yr$. These rates are higher than estimates of San Juan Mountain dust accumulation of 5-10 $g/m^2/yr$ and 22 $g/m^2/yr$ respectively (Lawrence et al., 2010, 2011). Higher deposition rates in Blue Lake likely reflect the influence of catchment and lake focusing. Blue Lake also suggests dust accumulation has varied on sub-decadal to millennial timescales over the last 4.5 millennia between nearly 0 and 120 $g/m^2/yr$.

Blue Lake dust accumulation followed a long-term decreasing trend since ca. 4500 BP, which reversed ca. 70 BP (1880 CE). Prior to human disturbance, dust emissions primarily reflect sediment source stability, which over the last 4.5 millennia was mediated in-part by aridity (Halfen et al., 2016). Dust deposition; however, is also influenced by wind strength and transport mechanisms. The long-term decreasing trend may have been driven in-part by long-term increases in effective moisture characterized regionally by Shuman et al. (2015), and more broadly by (Shuman & Marsicek, 2016).

There are several intervals of dustiness rising above the long-term trend related to sedimentation and chronology. The largest peak in dustiness is at ca. 1500 BP (450 CE). The 1500 BP peak occurs prior to the peak in dust concentrations (Figure 4B), and is driven by a moderate increase in sediment density in core B (Figure 4D) and a spike in sedimentation rates (Figure 4C). The change in sedimentation rate is part of a broader increase, but the peak coincides with two radiocarbon dates (one in core A and core B). The dates are based on a pine cone and a wood fragment that could have remained on the landscape for a long time before being deposited in the lake, thus potentially leading to anomalously older age. Another dust peak at ca. 3000 BP coincides with both increases in sedimentation rates and dust concentrations.

7

Drought has been well characterized in Western North America over the last two millennia (e.g. Cook et al., 2004), yet the connection between tree-ring records of drought and dust mass accumulation at Blue Lake is tenuous (Fig. 5a-d). The Medieval Period (1200-550 BP), as characterized by tree-rings, had increased drought frequency, intensity, duration, and area in Western North America (Cook et al., 2004; Woodhouse & Overpeck, 1998). Yet Blue Lake shows relatively low dust mass accumulation during this time (21.8 $g/m^2/yr$) with respect the long-term preindustrial average of 28.4 $g/m^2/yr$. Dust mass accumulation was only slightly higher than average during the Roman period (ca. 2000-1800 BP, 29.7 $g/m^2/yr$), which has been characterized by tree-rings as an interval of regionally extreme drought (Routson et al., 2011).

Testing the likelihood of increased dust during drought shows no significant difference in DMAR between drought years and non-drought years and similarly no significant difference between drought and non-drought 30-year periods (Fig. 5b). This result is consistent with a composite record from nearby lakes. However, 20% of age model ensembles suggest increased dust during drought years. As a result, we cannot rule out the possibility that drought is driving variability in dust deposition.

The apparent lack of coherence between drought as recorded by tree-rings and sedimentary records is widespread (Shuman et al., 2017). In the case of dust fluxes off the Colorado Plateau, sediment supply and transport mechanisms by storm systems and wet deposition play key roles that could be inversely or un-related to effective moisture (Lancaster, 1997b; Lawrence et al., 2010). Records of aeolian sediment suggests the Southwest deserts have been continuously close to the threshold of activity over the last 4000 years, with periods of activation centered around 1 and 2500 BP (Busacca et al., 2003). These activation periods of sediment supply are likely related first to changes in vegetation cover and river systems, in turn affected by seasonal rainfall. In addition, periods of greater deposition would not necessarily correlate with drought as transport mechanisms in winter today occur through storms 70% of the time (Lawrence et al., 2010) implying a role of atmospheric circulation. The dust deposition record is likely representing the synergy between sediment supply and transport mechanisms, as modulated by large scale atmospheric circulation.

Human disturbance coincides with an increase in dust accumulation rates from a low point of 18 $g/m^2/yr$ (1650 CE to 1900 CE average) to 49 $g/m^2/yr$ (1900 CE to 2009 CE average), representing a 2.8-fold increase. Over the late Holocene preindustrial accumulation average of 28 $g/m^2/yr$ (record average prior to 1900 CE), suggesting human disturbance increased dust mass accumulation rates 1.7-fold above the long-term preindustrial average. Recent dust mass accumulation rates as characterized in Blue Lake have declined from a maximum in ca. 1950 of 120 $g/m^2/yr$ to a 1980-2009 average of 43 $g/m^2/yr$. These increases in dust accumulation are smaller than those characterized by Neff et al. (2008) in the northern San Juan Mountains, but consistent with human induced dust increases globally (Hooper & Marx, 2018). This period of

8

increased dust deposition coincides with land-use intensification in the Southwest. A rapid increase in livestock numbers and a near doubling of irrigated farmland accompanied the completion of the trans-national railroad in the late 1800s (Abruzzi, 1995); activities that disturbed otherwise stable land surfaces and increasing sediment supply.

## 4. Conclusions

Blue Lake dust deposition has decreased on average between ca. 4500 yr BP and ca. 70 yr BP. The long-term trend was potentially driven by a long-term increase in winter moisture in western North America, identified in several sedimentary records, leading to enhanced soil stability and a reduction in dust emission in the source areas (Shuman et al., 2017). But the difference in DMAR between drought and non-drought intervals as recorded by trees on the Colorado Plateau is insignificant. Links between dust and drought are likely confounded by wind-strength, sediment supply, and vegetation. Blue Lake indicates human disturbance increased dust mass accumulation rates an average of 1.7 times above the background conditions. Long-term dust variability suggests the region is naturally prone to dustiness. Nonetheless, humans and livestock have dominated dust emissions over the past century, suggesting humans can largely mitigate future dust levels through land-use management.
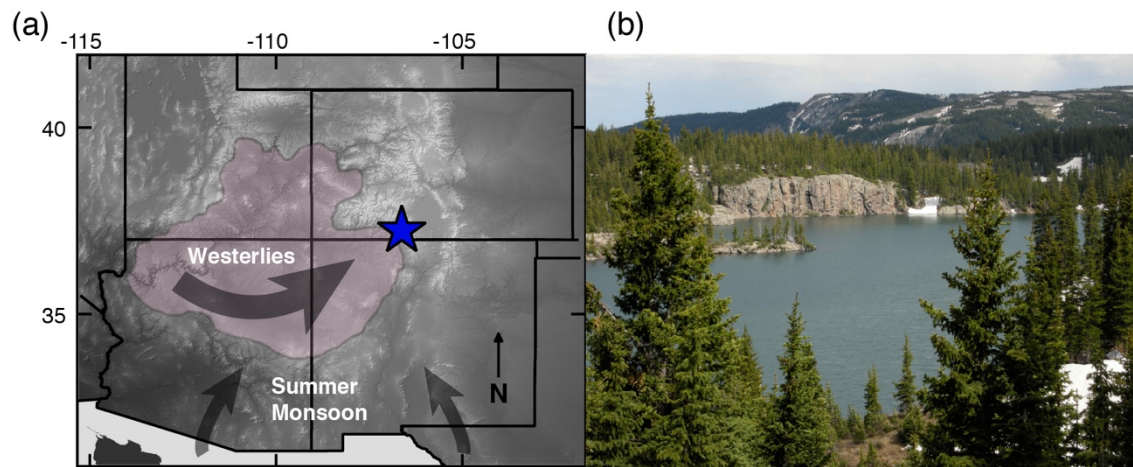
**Figures**

**Figure 1.** (a) Map showing the location of Blue Lake (blue star) with respect to the Colorado Plateau (shaded pink), and dominant circulation patterns (arrows). Westerly storm systems during the winter and spring are the dominant dust vector to the southern Rocky Mountains. (b) Overview photograph of Blue Lake.
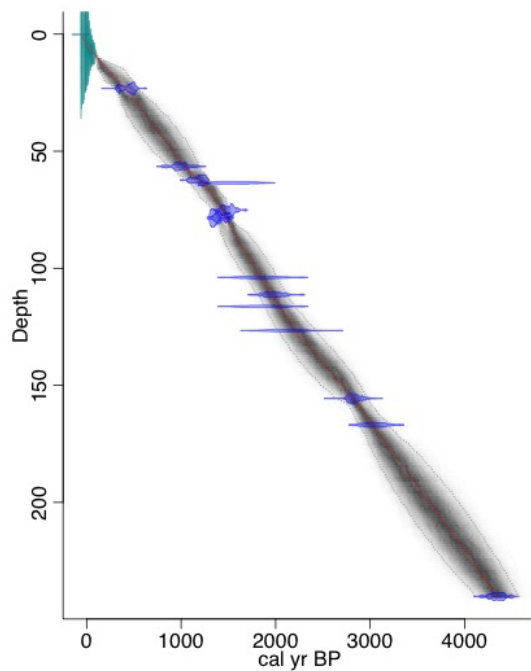
**Figure 2.** Age model including 16 $^{210}$Pb dates and 13 $^{14}$C dates computed using Bayesian Age depth program BACON (Blaauw et al., 2011). The width of the blue markers represents the age range and the height corresponds to the probability. The grey cloud shows the ensemble of possible age models, which has been incorporated into the reconstruction error below.
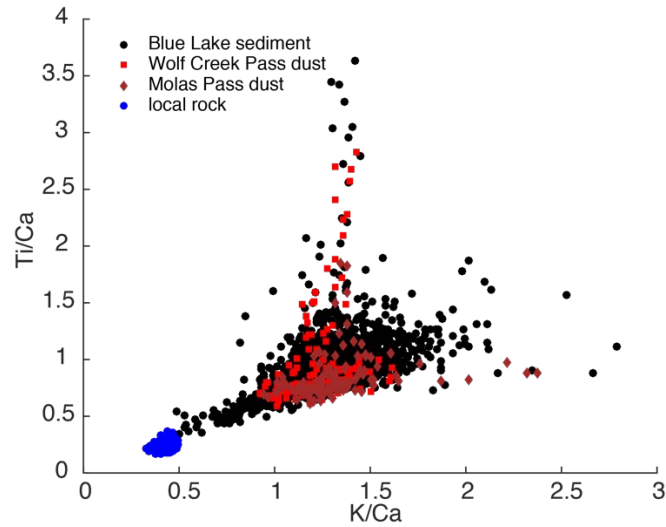


**Figure 3.** Elemental ratio-ratio scatter plot of Ti/Ca and K/Ca elemental ratios. Sediment (black) is a mixture of bedrock (blue) and dust (red) endmembers.
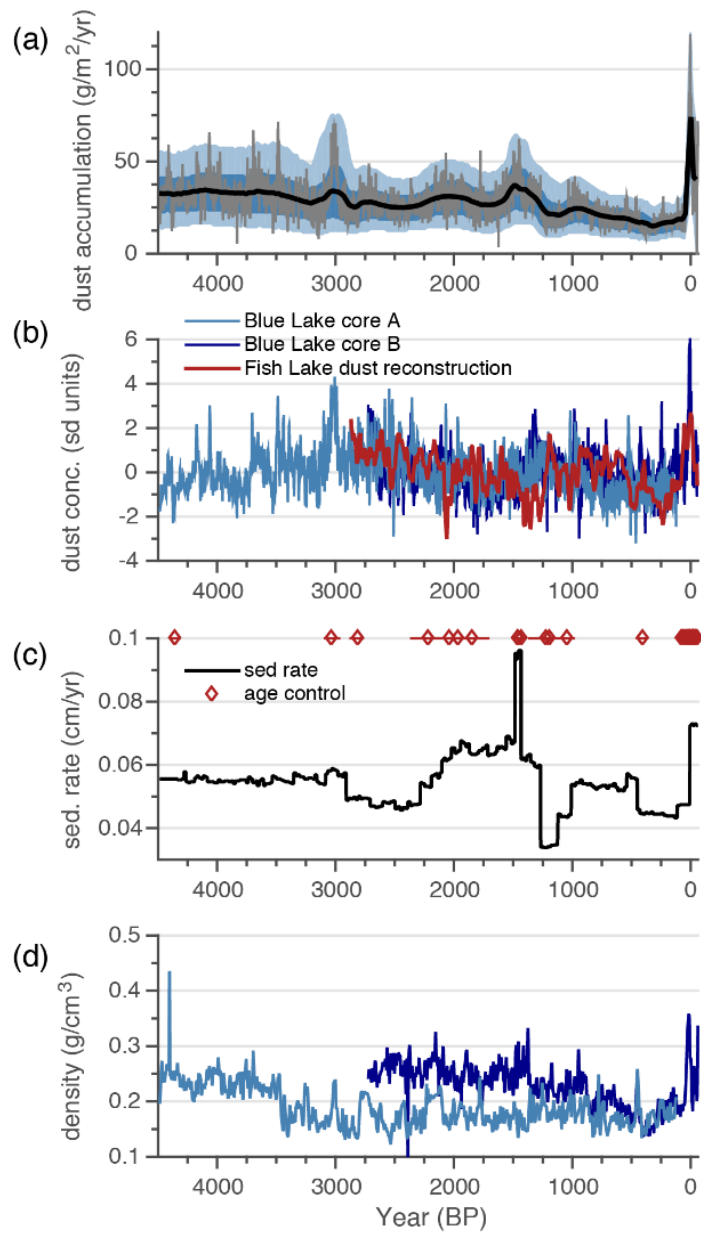
**Figure 4.** Blue Lake sediment dust mass accumulation reconstruction (a), which incorporates dust concentrations in the sediment cores (b), sedimentation rates (c), and sediment density (d). Fish Lake dust concentrations (b, red) are plotted with the Blue Lake dust concentrations (b, blue). Age control points are plotted in the diamonds in panel (c), showing the relationship between age control and changes in sedimentation rates.
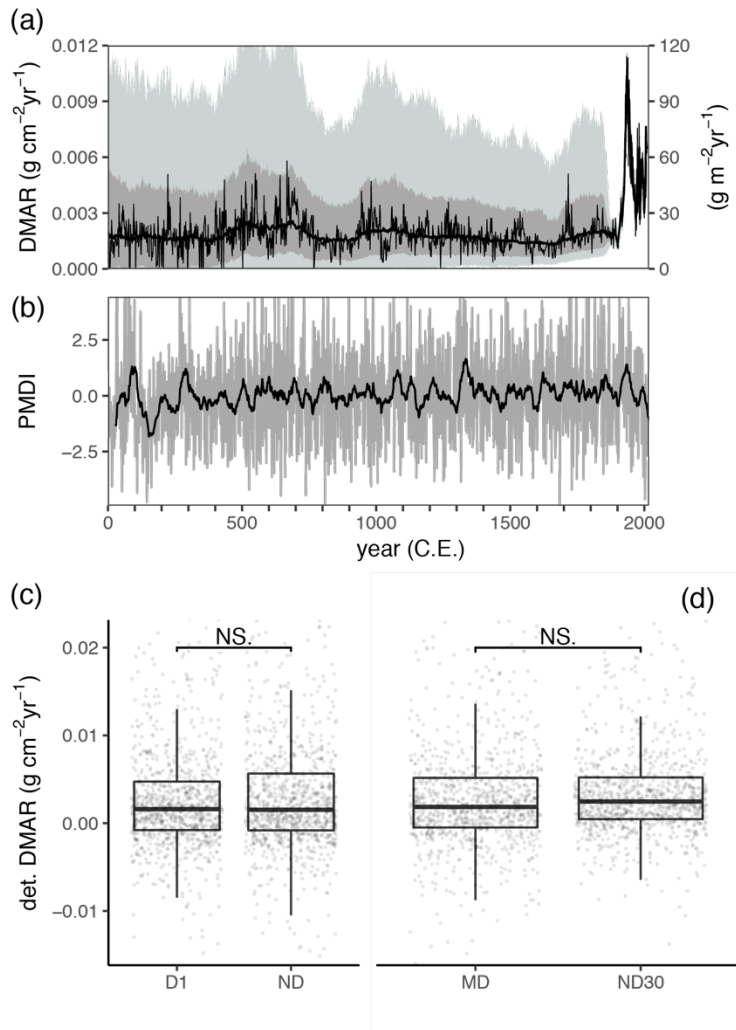
13

**Figure 5.** Detrended Blue Lake dust mass accumulation rates and uncertainties due to age uncertainty (a). Outer light-gray shading indicates the 95% highest density region, dark gray shows the inter-quartile range, and the smooth black line shows the median. A best estimate of DMAR is also shown in black. Palmer Modified Drought Index smoothed with a 30-year moving average (b). Boxplot of Blue Lake dust mass accumulation rate (DMAR) during drought years with Palmer Modified Drought Index (PMDI) < -1 (D1) as compared to years without drought conditions (ND; PMDI >= 0) (c). Multidecadal-length drought defined as a 30-year running average PMDI<-1 (MD) compared with 30-year running average PMDI >= 0 (ND30) (d). Significance in the difference in mean is indicated with N.S. for non-significant using the Wilcox

14

test. Sample size was accounted for by randomly selecting an equal number of years for each category. Points represent individual years or 30-year running averages with their own age model ensemble member.

**References:**

Abruzzi, W. S. (1995). The social and ecological consequences of early cattle ranching in the

Little Colorado River Basin. *Human Ecology*, *23*(1), 75–98.

https://doi.org/10.1007/BF01190099

Appleby, P. G., & Oldfield, F. (1983). The assessment of 210Pb data from sites with varying

sediment accumulation rates. In J. Meriläinen, P. Huttunen, & R. W. Battarbee (Eds.),

*Paleolimnology* (pp. 29–35). Springer Netherlands. Retrieved from

http://link.springer.com/chapter/10.1007/978-94-009-7290-2_5

Appleby, P. G., Nolan, P. J., Gifford, D. W., Godfrey, M. J., Oldfield, F., Anderson, N. J., &

Battarbee, R. W. (1987). 210Pb dating by low background gamma counting. In H. Löffler

(Ed.), *Paleolimnology IV* (pp. 21–27). Springer Netherlands. Retrieved from

http://link.springer.com/chapter/10.1007/978-94-009-4047-5_4

Ballantyne, A. P., Brahney, J., Fernandez, D., Lawrence, C. L., Saros, J., & Neff, J. C. (2011).

Biogeochemical response of alpine lakes to a recent increase in dust deposition in the

Southwestern, US. *Biogeosciences*, *8*(9), 2689–2706. https://doi.org/10.5194/bg-8-2689-

2011

Binford, M. W. (1990). Calculation and uncertainty analysis of 210Pb dates for PIRLA project

lake sediment cores. *Journal of Paleolimnology*, *3*(3), 253–267.

https://doi.org/10.1007/BF00219461

Blaauw, M., & Christen, J. A. (2011). Flexible paleoclimate age-depth models using an

autoregressive gamma process. *Bayesian Analysis*, *6*(3), 457–474.

https://doi.org/10.1214/ba/1339616472

Bullard, J. E., & Livingstone, I. (2002). Interactions between aeolian and fluvial systems in

dryland environments. *Area*, *34*(1), 8–16. https://doi.org/10.1111/1475-4762.00052

Busacca, A. J., Begét, J. E., Markewich, H. W., Muhs, D. R., Lancaster, N., & Sweeney, M. R.

(2003). Eolian sediments. In *Developments in Quaternary Sciences* (Vol. 1, pp. 275–309).

Elsevier. https://doi.org/10.1016/S1571-0866(03)01013-3

Cook, B. I., Ault, T. R., & Smerdon, J. E. (2015). Unprecedented 21st century drought risk in the

American Southwest and Central Plains. *Science Advances*, *1*(1), e1400082.

https://doi.org/10.1126/sciadv.1400082

Cook, E. R., Woodhouse, C. A., Eakin, C. M., Meko, D. M., & Stahle, D. W. (2004). Long-term

aridity changes in the western United States. *Science*, *306*(5698), 1015–1018.

https://doi.org/10.1126/science.1102586

Cook, E. R., Seager, R., Heim, R. R., Vose, R. S., Herweijer, C., & Woodhouse, C. (2010).

Megadroughts in North America: placing IPCC projections of hydroclimatic change in a

long-term palaeoclimate context. *Journal of Quaternary Science*, *25*(1), 48–61.

https://doi.org/10.1002/jqs.1303

Derbyshire, E. (2007). Natural minerogenic dust and human health. *AMBIO: A Journal of the Human Environment*, *36*(1), 73–77. https://doi.org/10.1579/0044-7447(2007)36[73:NMDAHH]2.0.CO;2

Ferrenberg, S., Reed, S. C., & Belnap, J. (2015). Climate change and physical disturbance cause similar community shifts in biological soil crusts. *Proceedings of the National Academy of Sciences*, 201509150. https://doi.org/10.1073/pnas.1509150112

Halfen, A. F., Lancaster, N., & Wolfe, S. (2016). Interpretations and common challenges of aeolian records from North American dune fields. *Quaternary International*, *410, Part B*, 75–95. https://doi.org/10.1016/j.quaint.2015.03.003

Hall, F. F. (1981). Visibility reductions from soil dust in the Western U.S. *Atmospheric Environment (1967)*, *15*(10), 1929–1933. https://doi.org/10.1016/0004-6981(81)90227-4

Hooper, J., & Marx, S. (2018). A global doubling of dust emissions during the Anthropocene? *Global and Planetary Change*, *169*, 70–91.
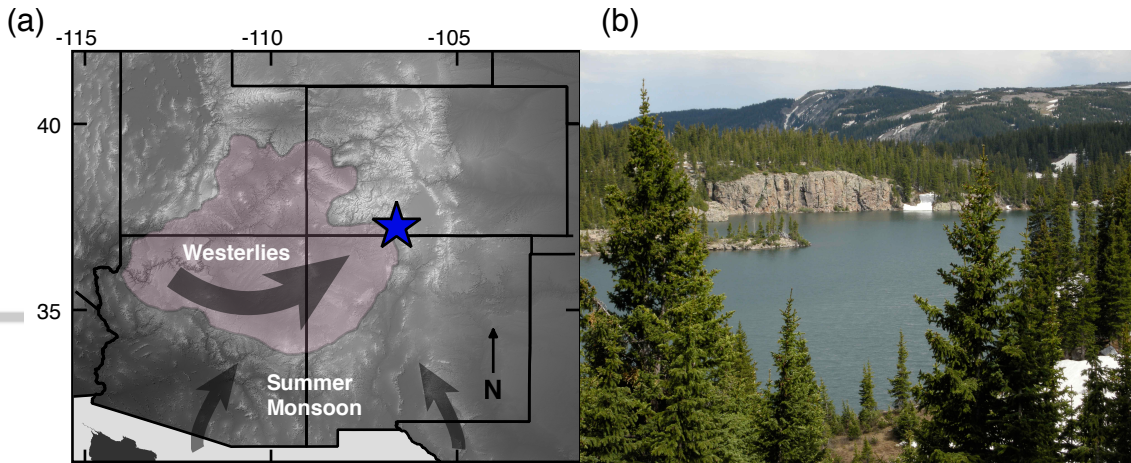
https://doi.org/10.1016/j.gloplacha.2018.07.003

Kok, J. F., Parteli, E. J. R., Michaels, T. I., & Karam, D. B. (2012). The physics of wind-blown sand and dust. *Reports on Progress in Physics*, *75*(10). https://doi.org/10.1088/0034-4885/75/10/106901
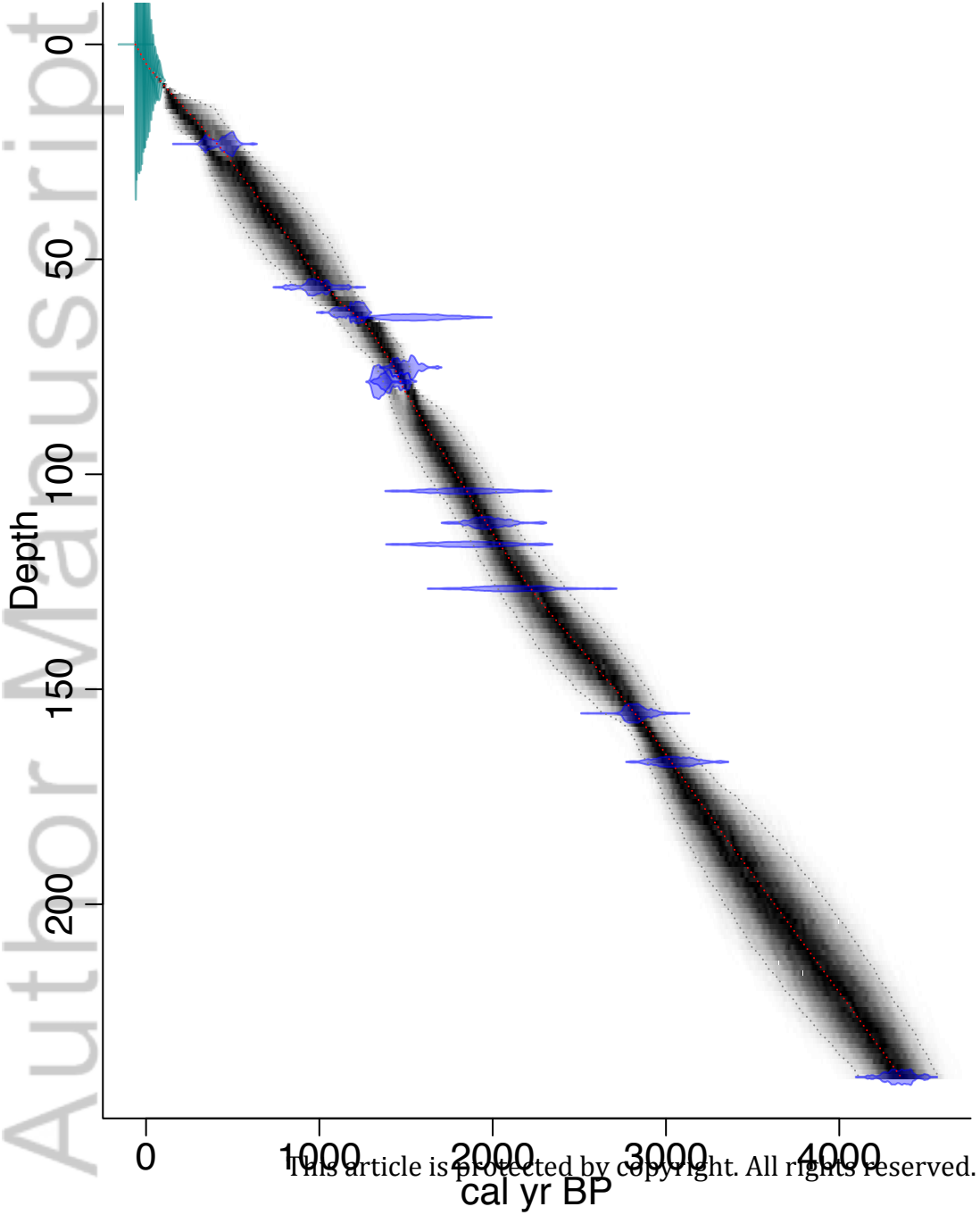
Krinner, G., Boucher, O., & Balkanski, Y. (2006). Ice-free glacial northern Asia due to dust deposition on snow. *Climate Dynamics*, *27*(6), 613–625. https://doi.org/10.1007/s00382-006-0159-z

Lancaster, N. (1997a). Response of eolian geomorphic systems to minor climate change: examples from the southern Californian deserts. *Geomorphology*, *19*, 333–347. https://doi.org/10.1016/S0169-555X(97)00018-4

Lawrence, C. R., Painter, T. H., Landry, C. C., & Neff, J. C. (2010). Contemporary geochemical composition and flux of aeolian dust to the San Juan Mountains, Colorado, United States. *Journal of Geophysical Research: Biogeosciences*, *115*(G3), G03007. https://doi.org/10.1029/2009JG001077

Lawrence, C. R., Neff, J. C., & Farmer, G. L. (2011). The accretion of aeolian dust in soils of the San Juan Mountains, Colorado, USA. *Journal of Geophysical Research: Earth Surface*, *116*(F2), F02013. https://doi.org/10.1029/2010JF001899

Li, J., Okin, G. S., Alvarez, L., & Epstein, H. (2007). Quantitative effects of vegetation cover on wind erosion and soil nutrient loss in a desert grassland of southern New Mexico, USA. *Biogeochemistry*, *85*(3), 317–332. https://doi.org/10.1007/s10533-007-9142-y

Lipman, P. W., & Hail, W. J. (1975). Reconnaissance geologic map of the Chama Peak quadrangle, Conejos and Archuleta. *U.S. Geologic Survey*. Retrieved from http://ngmdb.usgs.gov/Prodesc/proddesc_3817.htm

Munson, S. M., Belnap, J., & Okin, G. S. (2011). Responses of wind erosion to climate-induced vegetation changes on the Colorado Plateau. *Proceedings of the National Academy of Sciences*, *108*(10), 3854–3859. https://doi.org/10.1073/pnas.1014947108

Nauman, T. W., Duniway, M. C., Webb, N. P., & Belnap, J. (2018). Elevated aeolian sediment transport on the Colorado Plateau, USA: The role of grazing, vehicle disturbance, and increasing aridity. *Earth Surface Processes and Landforms*, *43*(14), 2897–2914. https://doi.org/10.1002/esp.4457

Neff, J. C., Ballantyne, A. P., Farmer, G. L., Mahowald, N. M., Conroy, J. L., Landry, C. C., et al. (2008a). Increasing eolian dust deposition in the western United States linked to human activity. *Nature Geoscience*, *1*(3), 189–195. https://doi.org/10.1038/ngeo133

Neff, J. C., Reynolds, R. L., Munson, S. M., Fernandez, D., & Belnap, J. (2013). The role of dust storms in total atmospheric particle concentrations at two sites in the western U.S. *Journal of Geophysical Research Atmospheres*, *118*(19), 11201–11212. https://doi.org/10.1002/jgrd.50855

Painter, Skiles S. McKenzie, Deems Jeffrey S., Brandt W. Tyler, & Dozier Jeff. (2017). Variation in rising limb of Colorado River snowmelt runoff hydrograph controlled by dust radiative forcing in snow. *Geophysical Research Letters*, *45*(2), 797–808. https://doi.org/10.1002/2017GL075826

19

Painter, T. H., Barrett, A. P., Landry, C. C., Neff, J. C., Cassidy, M. P., Lawrence, C. R., et al. (2007). Impact of disturbed desert soils on duration of mountain snow cover. *Geophysical Research Letters*, *34*(12), L12502. https://doi.org/10.1029/2007GL030284

Painter, T. H., Deems, J. S., Belnap, J., Hamlet, A. F., Landry, C. C., & Udall, B. (2010a). Response of Colorado River runoff to dust radiative forcing in snow, (5). https://doi.org/10.1073/pnas.0913139107

Reimer, P. J., Bard, E., Bayliss, A., Beck, J. W., Blackwell, P. G., Ramsey, C. B., et al. (2013). IntCal13 and Marine13 radiocarbon age calibration curves 0–50,000 years cal BP. *Radiocarbon*, *55*(4), 1869–1887. https://doi.org/10.2458/azu_js_rc.55.16947

Reynolds, R. L., Mordecai, J. S., Rosenbaum, J. G., Ketterer, M. E., Walsh, M. K., & Moser, K. A. (2009). Compositional changes in sediments of subalpine lakes, Uinta Mountains (Utah): evidence for the effects of human activity on atmospheric dust inputs. *Journal of Paleolimnology*, *44*(1), 161–175. https://doi.org/10.1007/s10933-009-9394-8

Routson, C. C., Woodhouse, C. A., & Overpeck, J. T. (2011). Second century megadrought in the Rio Grande headwaters, Colorado: How unusual was medieval drought? *Geophysical Research Letters*, *38*(22), L22703. https://doi.org/10.1029/2011GL050015

Routson, C. C., Overpeck, J. T., Woodhouse, C. A., & Kenney, W. F. (2016a). Three millennia of southwestern North American dustiness and future implications. *PLOS ONE*, *11*(2), e0149573. https://doi.org/10.1371/journal.pone.0149573

Schelske, C. L., Peplow, A., Brenner, M., & Spencer, C. N. (1994). Low-background gamma

    counting: applications for210Pb dating of sediments. *Journal of Paleolimnology*, *10*(2),

    115–128. https://doi.org/10.1007/BF00682508

Shuman, B. N., Routson, C., McKay, N., Fritz, S., Kaufman, D., Kirby, M. E., et al. (2017).

    Millennial-to-centennial patterns and trends in the hydroclimate of North America over

    the past 2000 years. *Clim. Past Discuss.*, *2017*, 1–33. https://doi.org/10.5194/cp-2017-35

Shuman, Bryan N., & Marsicek, J. (2016). The structure of Holocene climate change in mid-

    latitude North America. *Quaternary Science Reviews*, *141*.

    https://doi.org/10.1016/j.quascirev.2016.03.009

Shuman, Bryan N., Pribyl, P., & Buettner, J. (2015). Hydrologic changes in Colorado during the

    mid-Holocene and Younger Dryas. *Quaternary Research*, *84*(2), 187–199.

    https://doi.org/10.1016/j.yqres.2015.07.004

Skiles, S. M., Painter, T. H., Belnap, J., Holland, L., Reynolds, R. L., Goldstein, H. L., & Lin, J.

    (2015). Regional variability in dust-on-snow processes and impacts in the Upper

    Colorado River Basin. *Hydrological Processes*, *29*(26), 5397–5413.

    https://doi.org/10.1002/hyp.10569

Woodhouse, C. A., & Overpeck, J. T. (1998). 2000 Years of drought variability in the central

    United States. *Bulletin of the American Meteorological Society*, *79*(12), 2693–2714.

    https://doi.org/10.1175/1520-0477(1998)079<2693:YODVIT>2.0.CO;2

22

(a)

dust accumulation (g/m²/yr)

(b)

dust conc. (sd units)

Blue Lake core A
Blue Lake core B
Fish Lake dust reconstruction

(c)

sed. rate (cm/yr)

sed rate
age control

(d)

density (g/cm³)

Year (BP)